

Supplementary material

Ivan Osorio-Leon¹, Camille Bouchez¹, Eliot Chatton¹, Nicolas Lavenant¹,
Laurent Longuevergne¹, Tanguy Le Borgne¹

¹Univ Rennes – CNRS, Géosciences Rennes - UMR 6118. Rennes, France

1 Data availability

Data for this paper is available in the Hplus database by following the permanent link <https://hplus.ore.fr/en/osorio-leon-et-al-2022-wrr-data>

2 Input compositions of water and rock for the base case simulation with the numerical model

Table 1. Input water composition for the numerical model

Temperature [°C]	16	
pH	7	
	Concentrations	[mol/kg]
$O_2(aq)$	2.6×10^{-2}	
Cl^-	1.9×10^{-3}	
SO_4^{2-}	3.0×10^{-4}	
Na^+	2.2×10^{-3}	
Mg^{2+}	5.3×10^{-4}	
Al^{3+}	8.9×10^{-8}	
H_4SiO_4	2.2×10^{-4}	
K^+	9.2×10^{-5}	
Ca^{2+}	2.5×10^{-4}	
Fe^{2+}	0.0	
$CO_2(aq)$	4.3×10^{-5}	

3 Mineral stability diagram

4 Dissolved iron measurements

Major and trace cations were quantified by Inductively Coupled Plasma Mass Spectroscopy (Agilent Technologies, 7700x) in pre-acidified and 0.2 μm -filtered samples. Uncertainties were between 2 to 5%. Major anion samples (non-acidified) were analyzed by Ionic Chromatography (Dionex DX-120) with uncertainties below 4%. Groundwater sampling consisted on descending a submersible MP1 pump (Grundfos) until the depth of the dominant fracture in the borehole. Physicochemical parameters in the pump discharge were monitored with a WTW probe. Groundwater was sampled after the monitored parameters were stable.

Corresponding author: Ivan-David Osorio-Leon, ivan-david.osorio-leon@univ-rennes1.fr

Corresponding author: Camille Bouchez, camille.bouchez@univ-rennes1.fr

Table 2. Mineralogical composition used as input for the numerical simulations. *Diss Only* indicates that only dissolution is allowed and *tst* indicates that both dissolution and precipitation can occur. Kinetic and thermodynamic parameters for Equation (4) are taken from the database files of the Thermoddem project (Blanc et al., 2012) and from Palandri and Kharaka (2004).

Mineral	Structural formula	Mineral volume fraction [Φ_j]	Reaction type
<i>Primary minerals</i>			
Albite	$NaAlSi_3O_8$	0.000	TST - Diss only
Quartz	SiO_2	0.444	TST - Diss only
K-Feldspar	$KAlSi_3O_8$	0.297	TST - Diss only
Biotite	$K(Mg_2Fe^{II})(Si_3Al)O_{10}(OH)_2$	0.099	TST - Diss only
Muscovite	$KAl_2(AlSi_3O_{10})(OH)_2$	0.149	TST - Diss only
<i>Secondary minerals</i>			
Chlorite	$(Mg_3Fe_2^{II}Al)(Si_3Al)O_{10}(OH)_8$	1×10^{-5}	TST
Kaolinite	$Al_2Si_2O_5(OH)_4$	0.000	TST
Goethite	$Fe^{III}OOH$	0.000	TST

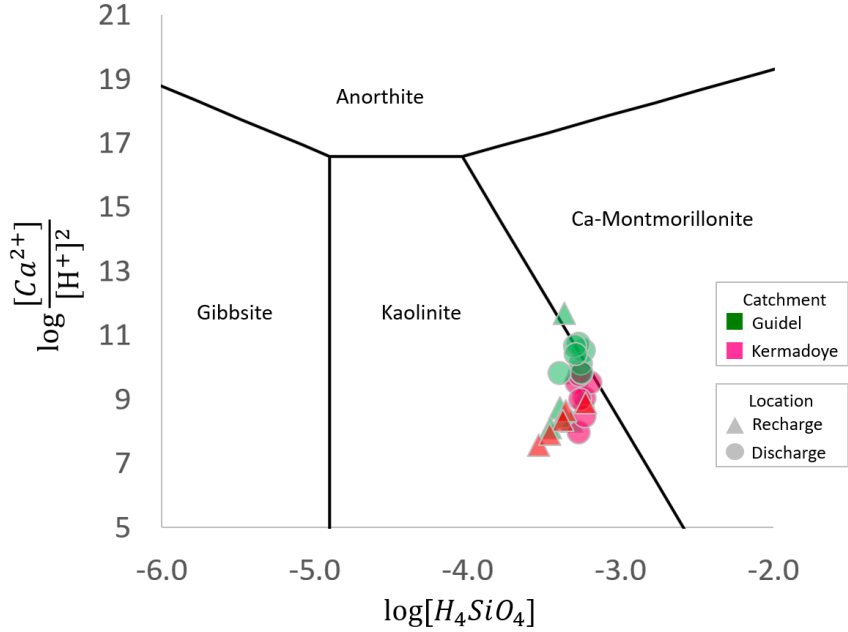


Figure 1. Mineral stability diagram

5 Depth of the groundwater reservoir

Since fracture networks are highly heterogeneous features (Le Borgne et al., 2006), one cannot directly rely the depth of an intersected fracture in a borehole with the representative depth of the circulating fluid’s reservoir. For instance, at the site scale, normal faults dipping of about 70° (Ruelleu et al., 2010) will globally favor subvertical circulations. At a more restricted scale, a fracture analysis in a borehole from the Guidel catchment (Bochet et al., 2020) has shown that fracture’s dip can vary from 20 to 80° .

Following this, we have used the groundwater’s temperature as a proxy of depth. Hence, the depth of the reservoir of the groundwater circulating in a fracture ($Depth_{proxy}$) was calculated as:

$$Depth_{proxy} = \frac{T - T_{rech}}{G_G}$$

T corresponds to groundwater temperature as measured from borehole logs, T_{rech} corresponds to the average recharge temperature of the Ploemur site, that is 12 °C, as deduced from the average temperature in the weather station, and G_G corresponds to the Geothermal Gradient. For the Ploemur site, G_G has been considered as 0.013 °C.m⁻¹ after (Pouladi et al., 2021).

6 Sensitivity of $Depth_{proxy}$ estimates

We note that the depth estimates for the DO measurements presented in Figure 7 rely on using groundwater’s temperature as a proxy for depth ($Depth_{proxy}$). As estimated, $Depth_{proxy}$ depends on two site-dependent parameters, i.e. the average recharge temperature (T_{rech}) and the Geothermal Gradient (G_G). Both parameters are mostly invariant at short timescales and are not easily measurable. As a result, uncertainties around their value come from measurements rather than seasonality or natural disturbances. The CZO of Ploemur is a well-studied site and both T_{rech} and G_G are well constrained, allowing to reduce uncertainty’s around their value. The average value for T_{rech} has been estimated to be 12.2±0.41 °C as deduced from temperature time-series (from 2002 to 2018) recorded at the weather station in the Ploemur CZO. On the other hand, previous works suggest that the G_G of the Ploemur site ranges between 0.016 and 0.013 °C.m⁻¹ (Pouladi et al., 2021; Klepikova et al., 2011) and for this work we considered the most recent estimate of 0.013 °C.m⁻¹ after Pouladi et al. (2021).

It is important to notice that the estimated $Depth_{proxy}$ is highly sensitive to both parameters and it can thus directly impact the estimated depth of the oxygenated zone in the aquifer. For instance, if one considers the borehole with the highest temperature (and thus the deepest $Depth_{proxy}$) from Figure 7 (from main text), and by combining the uncertainties of T_{rech} and G_G , the maximum depth in which oxygen has been detected in this study can oscillate between 333 m and 473 m below surface.

6.1 Effect of velocity on oxic iron concentrations

Figure 2 shows how, for a same Damköhler number, the variations in the apparent vertical velocity impacts the iron concentrations at oxic conditions according to Equation 19 in main text. Predicted concentrations are restricted to low values because they are limited by the fast oxidation of iron by oxygen. Note that they are close to the detection limit of ICPMS analysis that usually is close to 10⁻⁴ ppb. This makes difficult to constrain the apparent vertical velocity by using the iron concentration data, yet it is possible if analytical methods for iron are sensible enough.

7 Borehole logs

7.1 Methods

Multiparameter borehole logs under ambient conditions (dissolved oxygen, temperature, electrical conductivity and pH) acquired since 2003, available in the database of the French network of hydrogeological research sites (<https://hplus.ore.fr/en/>), were used as base for exploring the physicochemical parameters with depth. This dataset was completed with two additional field campaigns in order to validate the historical data. Multiparameter borehole logs in ambient conditions were acquired at two different times of the hydrologic year: high groundwater level’s season (late fall 2022) and low level’s season (late spring 2021) using an Idronaut Ocean Seven multiparameter probe. The instrument was calibrated following the manufacturer’s specification and the accuracy of

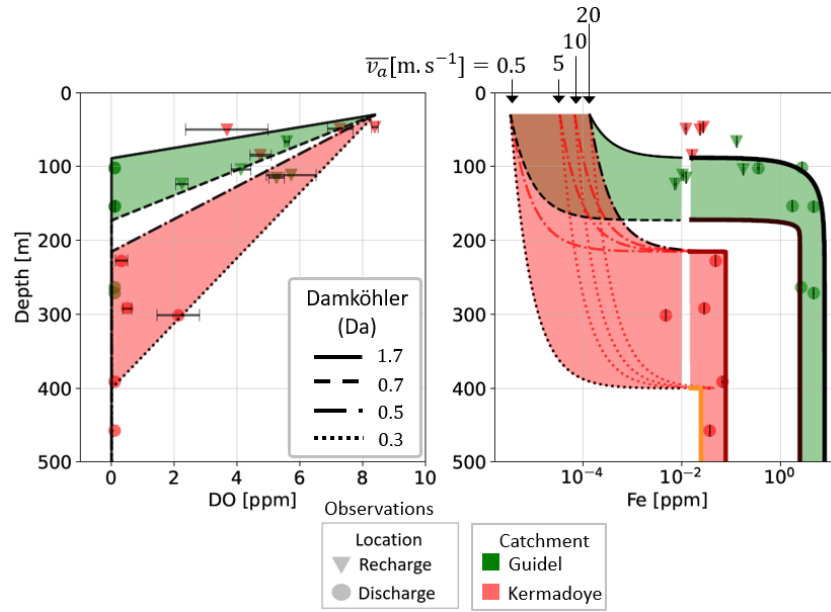


Figure 2. Effect of vertical velocity on the predicted iron concentrations at oxic concentrations

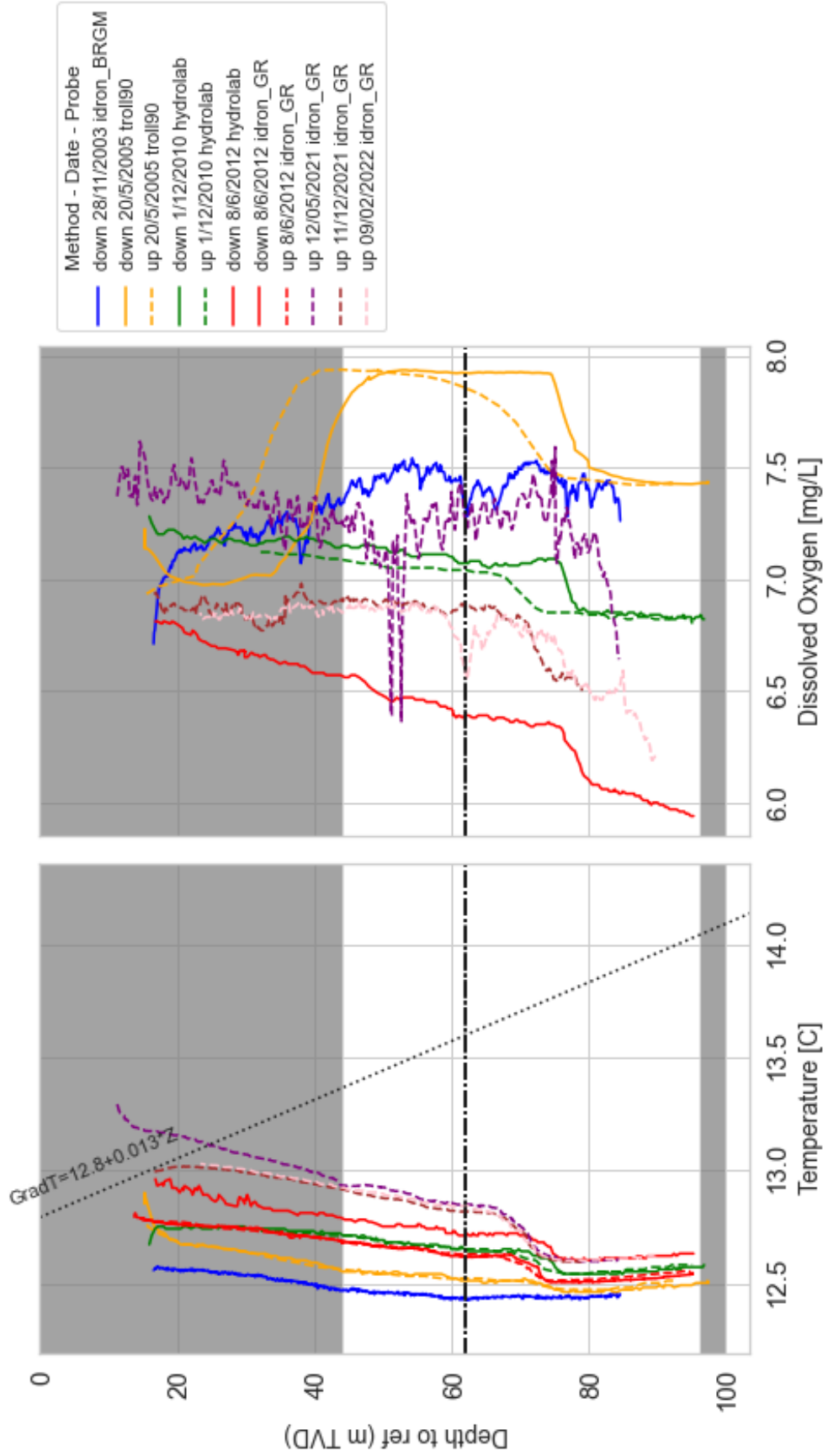
75 the DO probe ($\pm 0.1 \text{ mg.L}^{-1}$) was crosschecked by gas chromatography analyses at the
 76 University of Rennes 1 (Figure 3).

77 7.2 logs per borehole

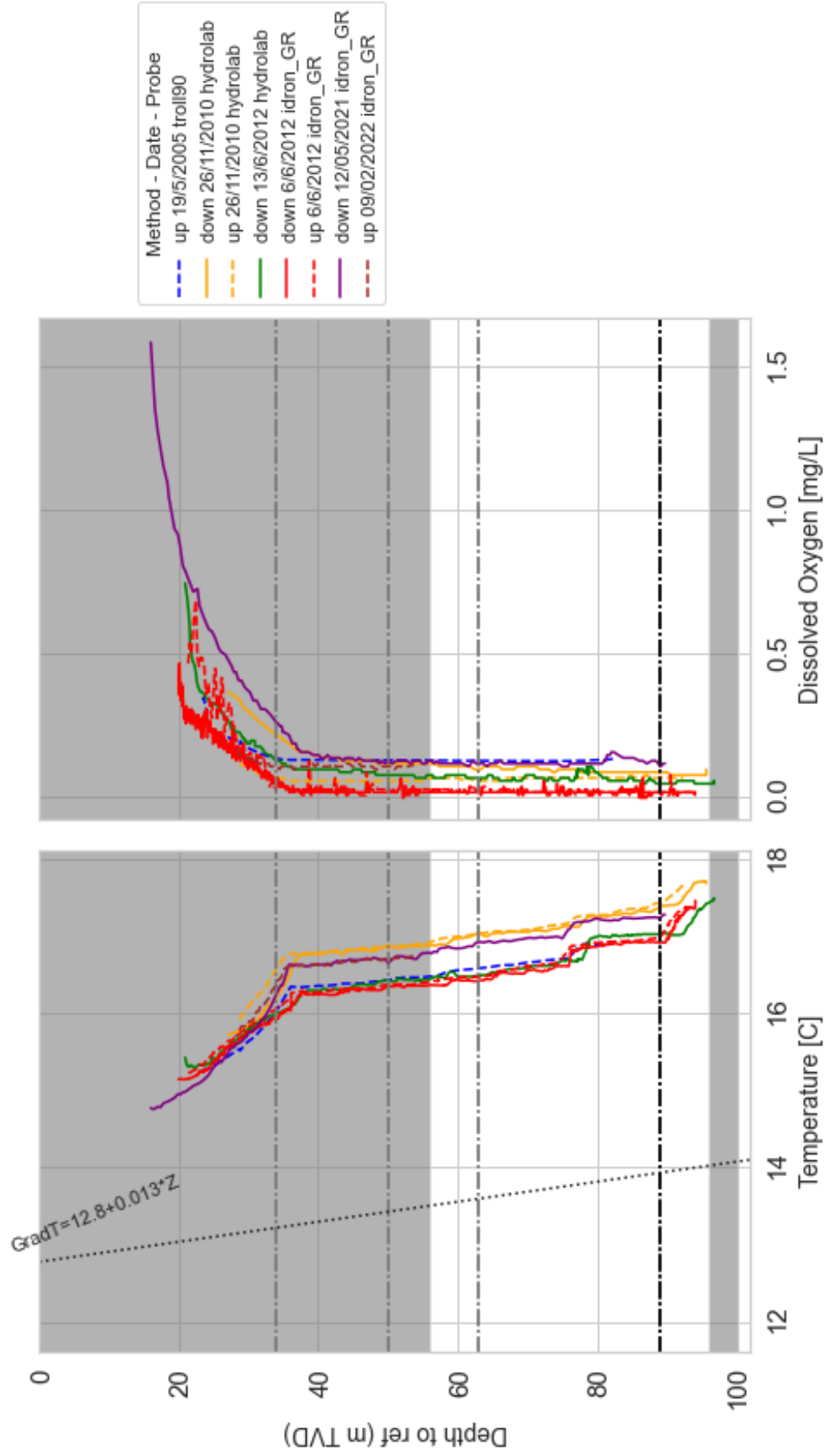
78 The following figures present the synthesis of multiparameter logs for every bore-
 79 hole. The shaded areas correspond to the tubewall while the white areas correspond the
 80 slotted sections. The horizontal dash-dotted lines correspond to fractures intersected in
 81 the borehole (black for the main fracture, grey for secondary fractures).

82 The legend in every plot indicate the mode of log-acquisition ("up" for upwards,
 83 down for "downwards"), the date, and the name of the multiparameter probe.

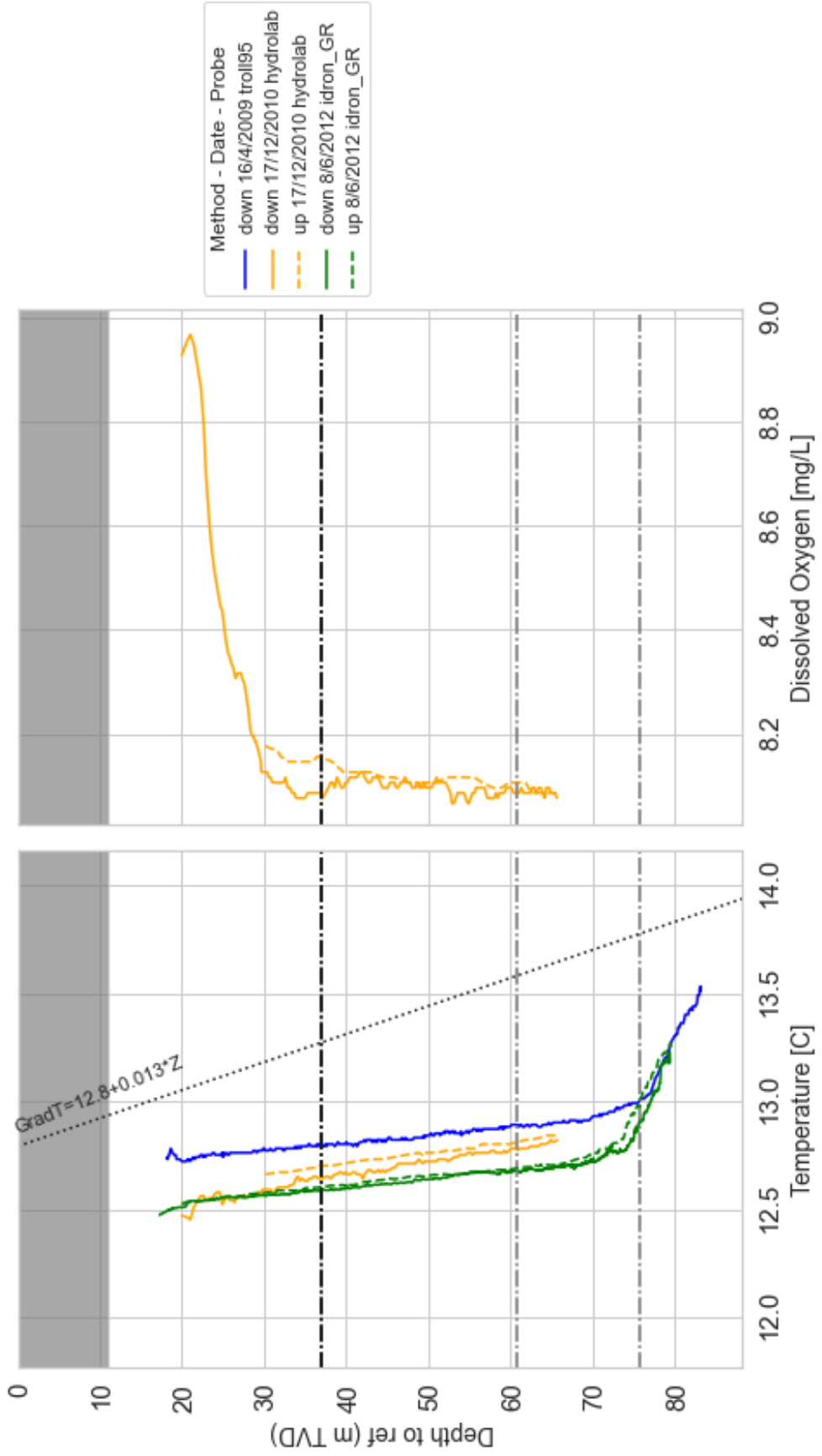
f9



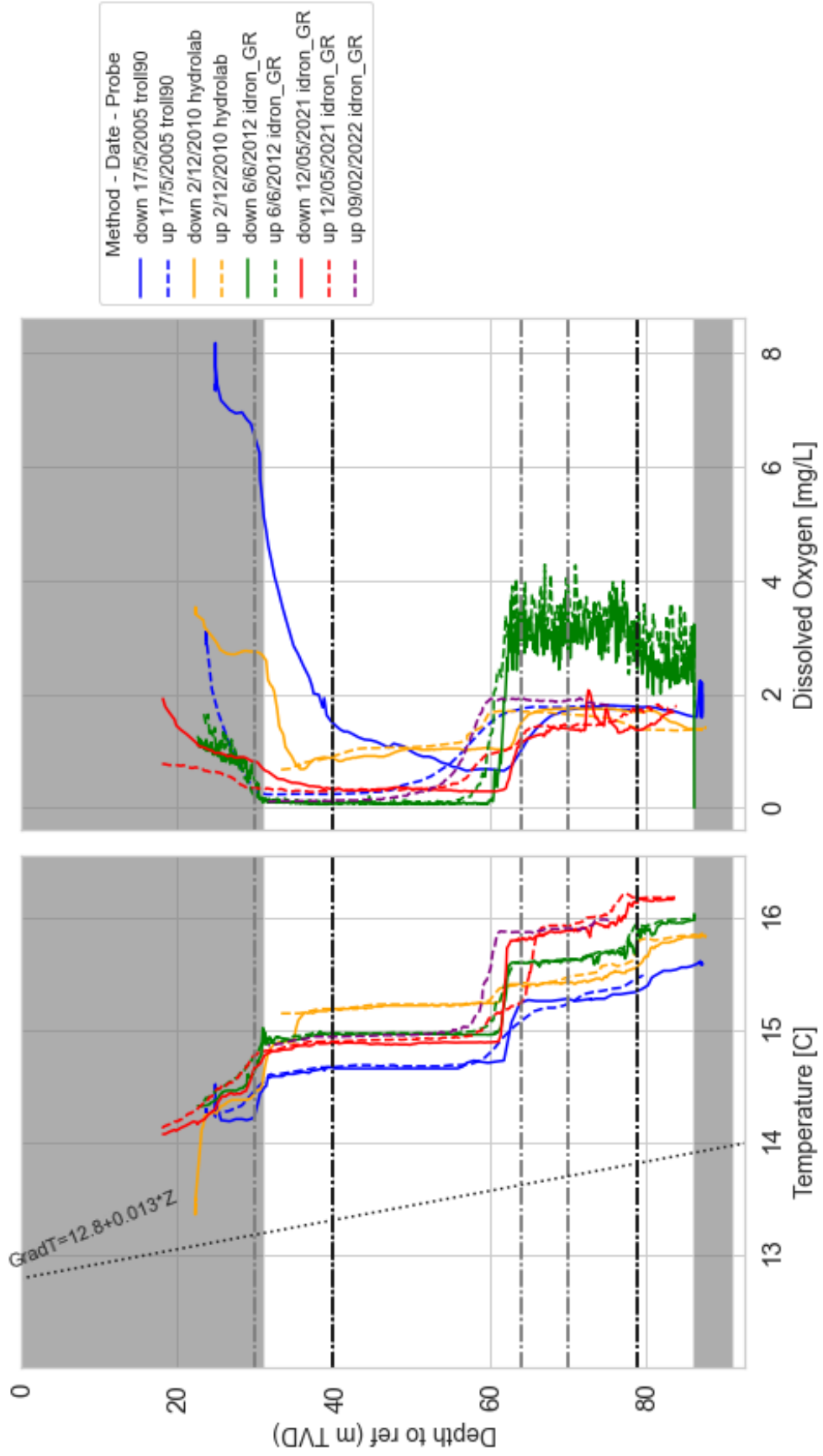
f11



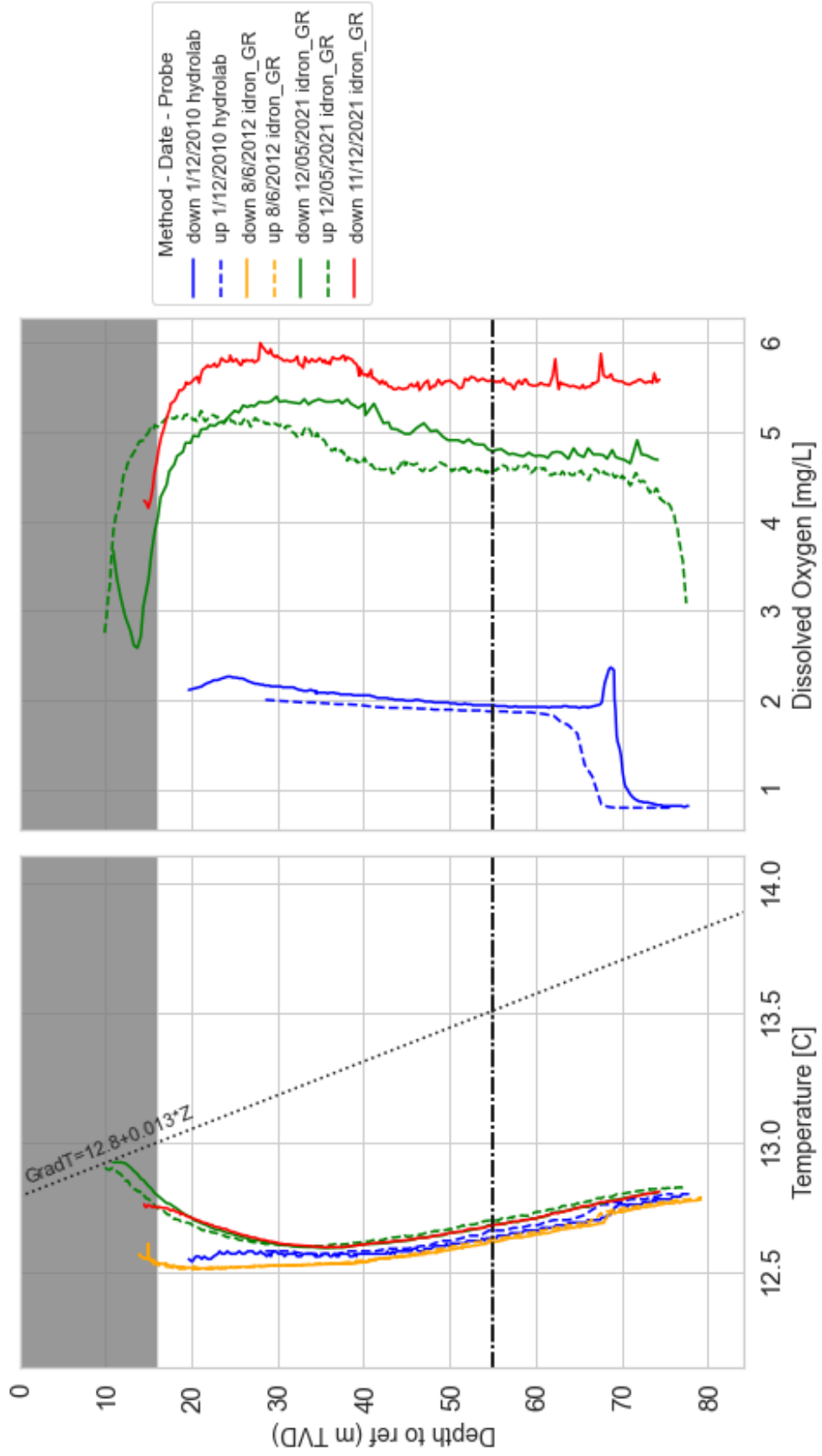
f20



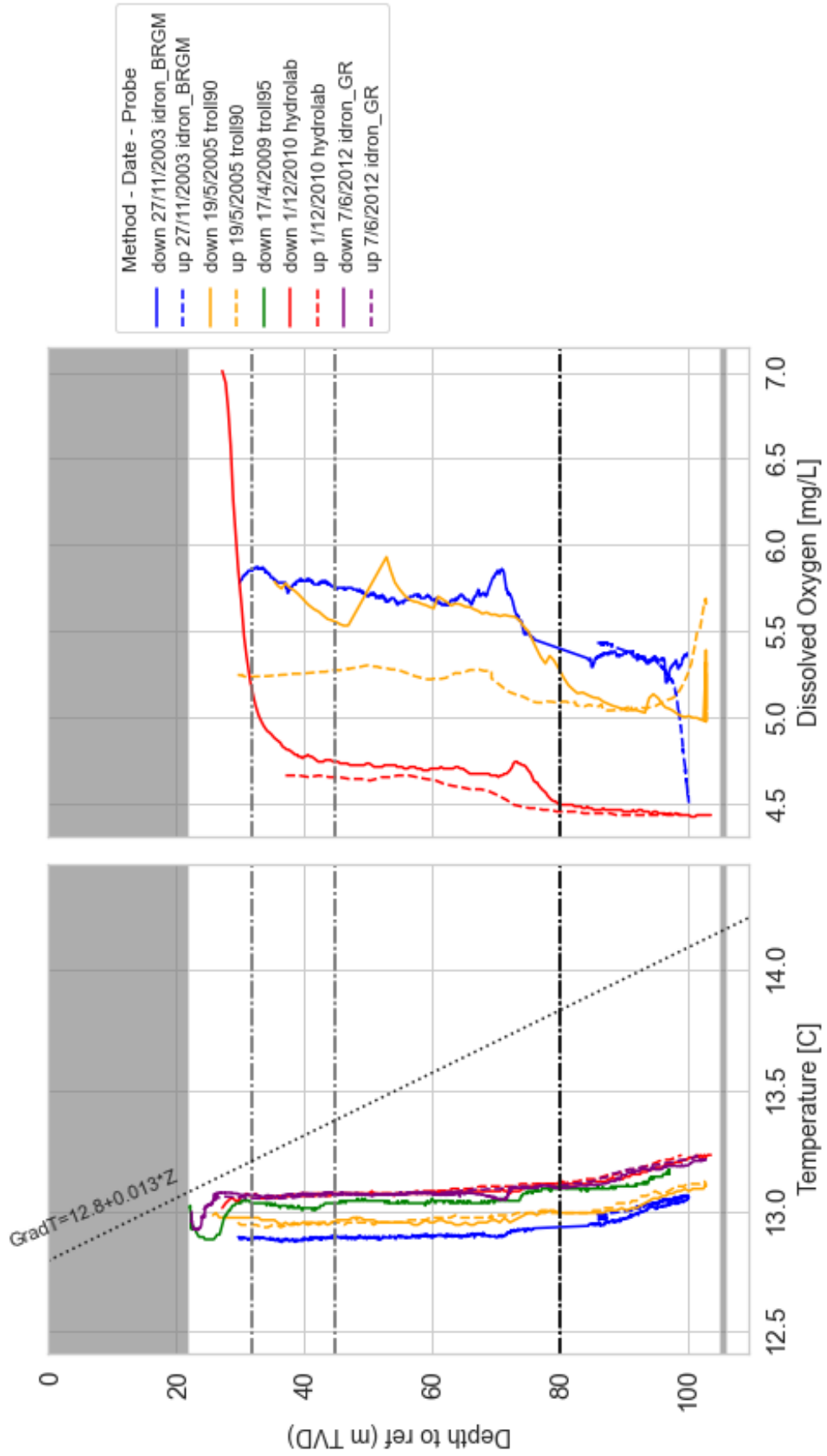
f28



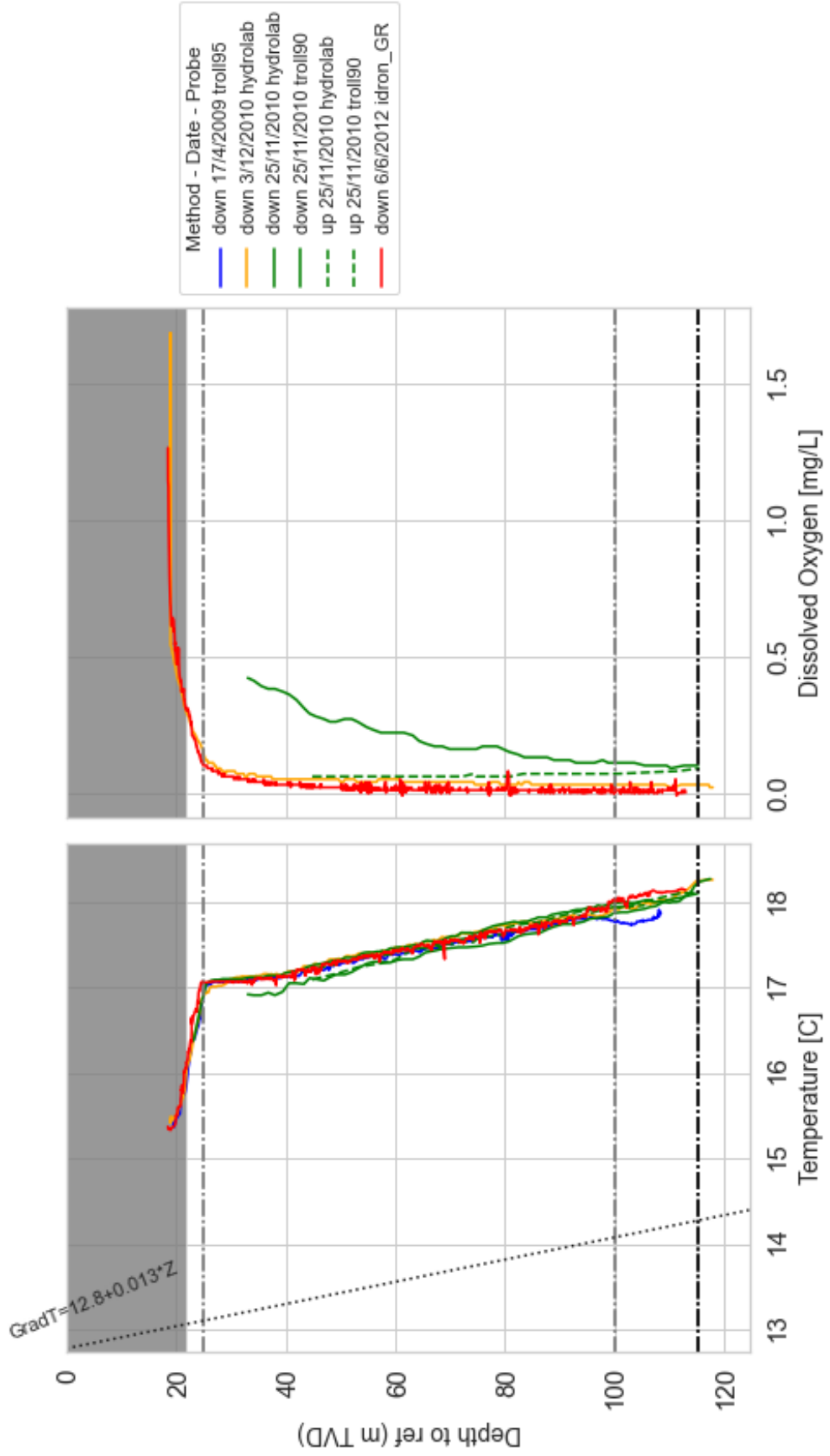
f30



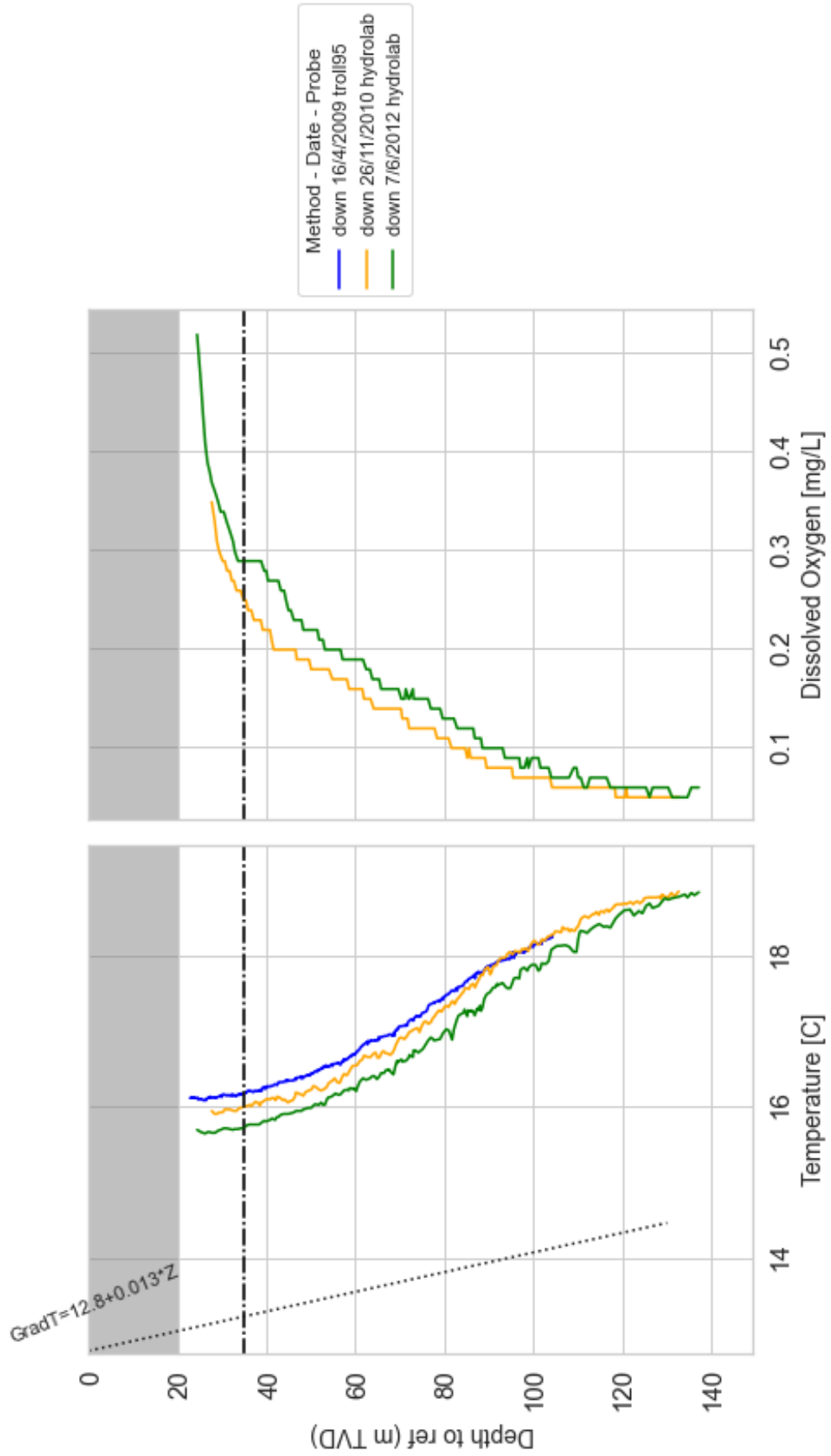
f34



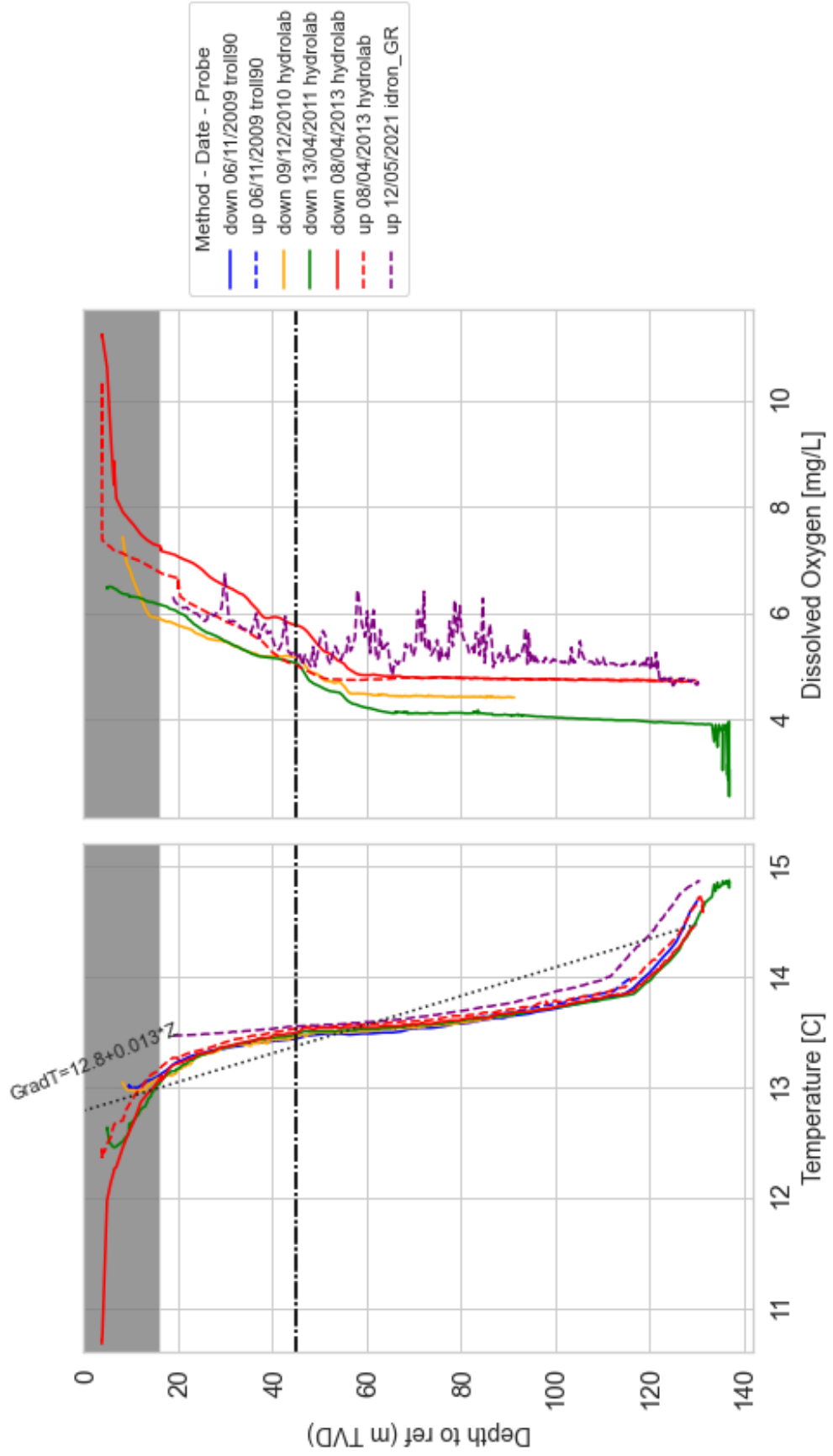
f37



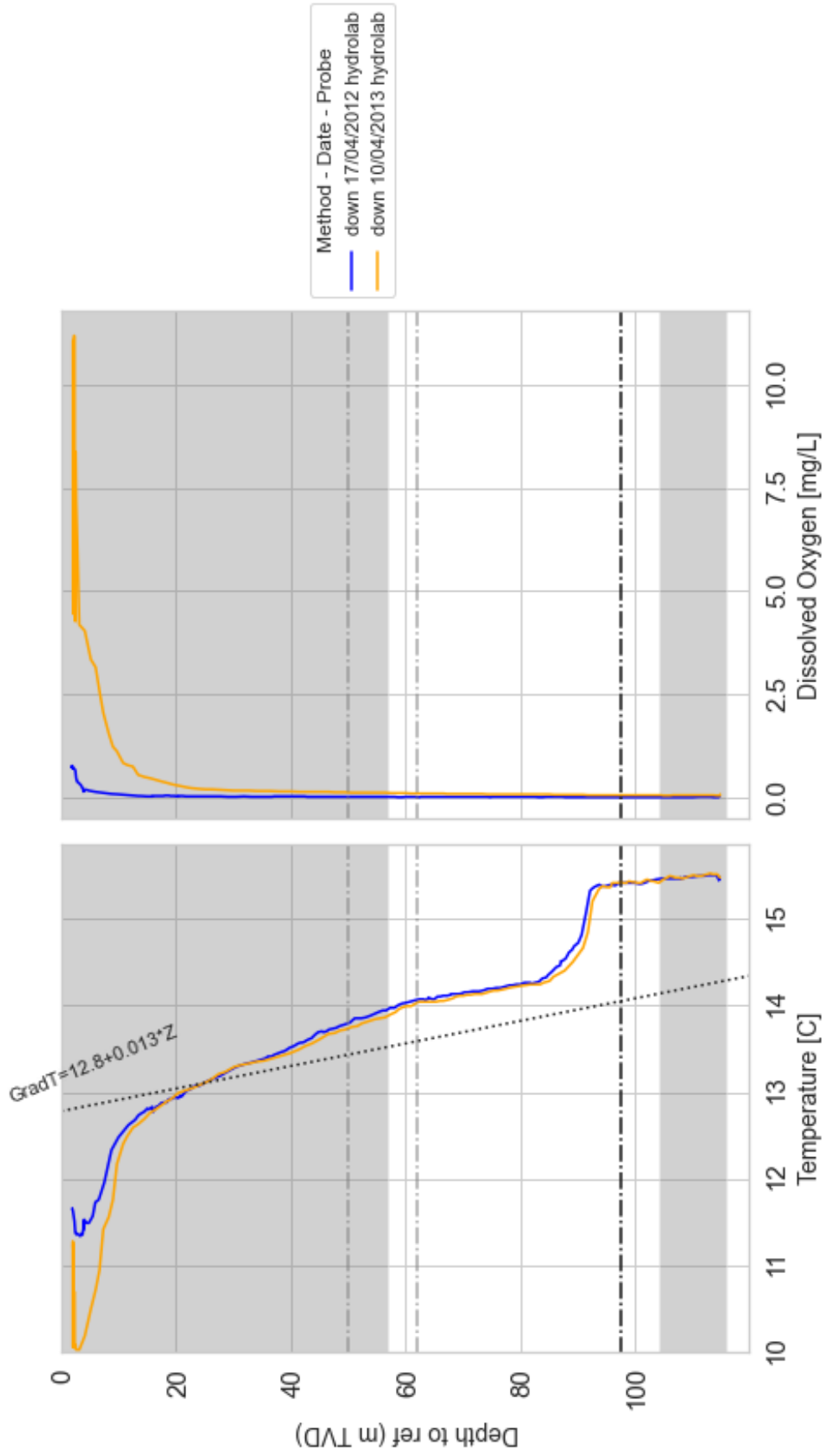
f38



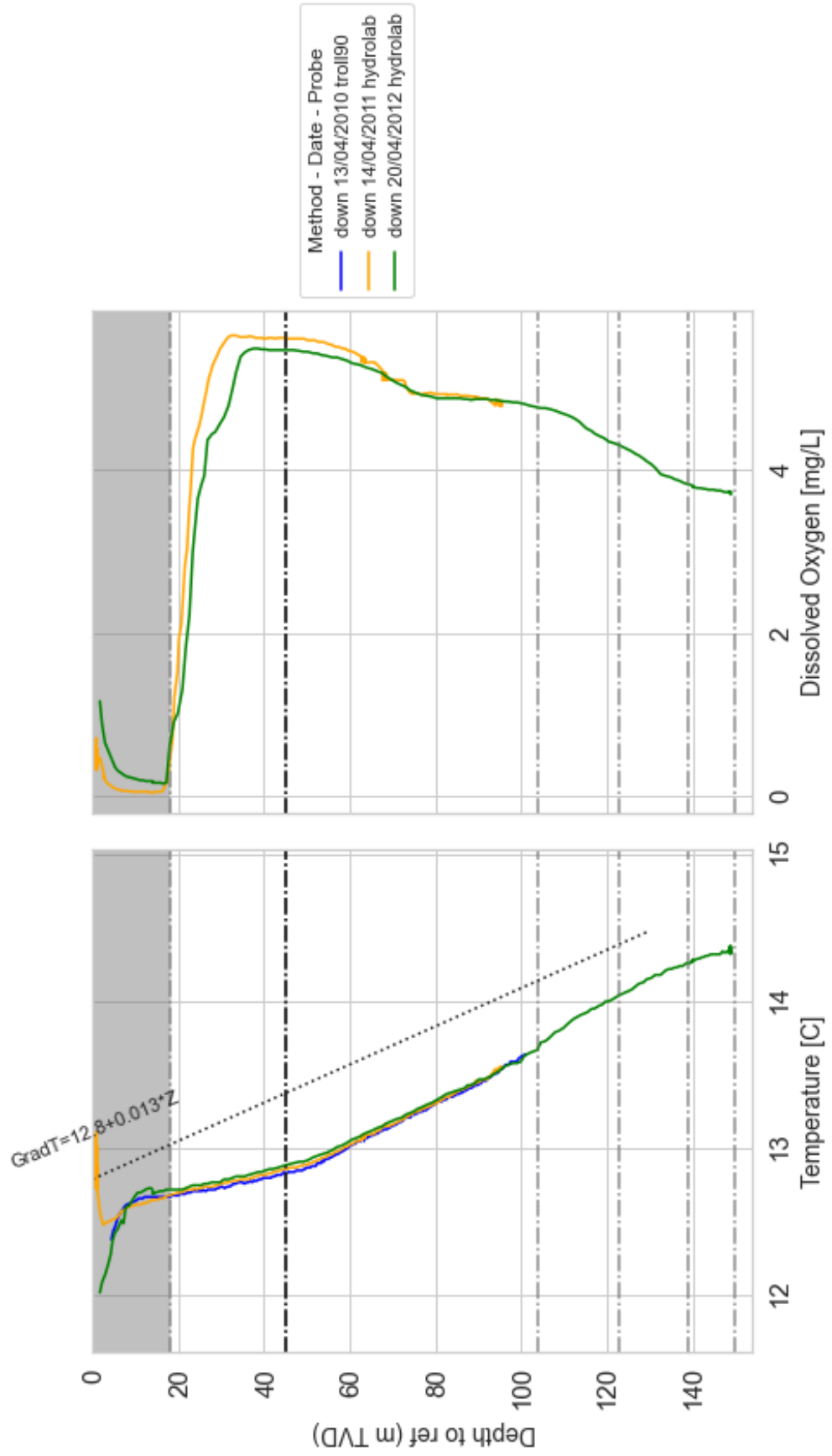
psr1

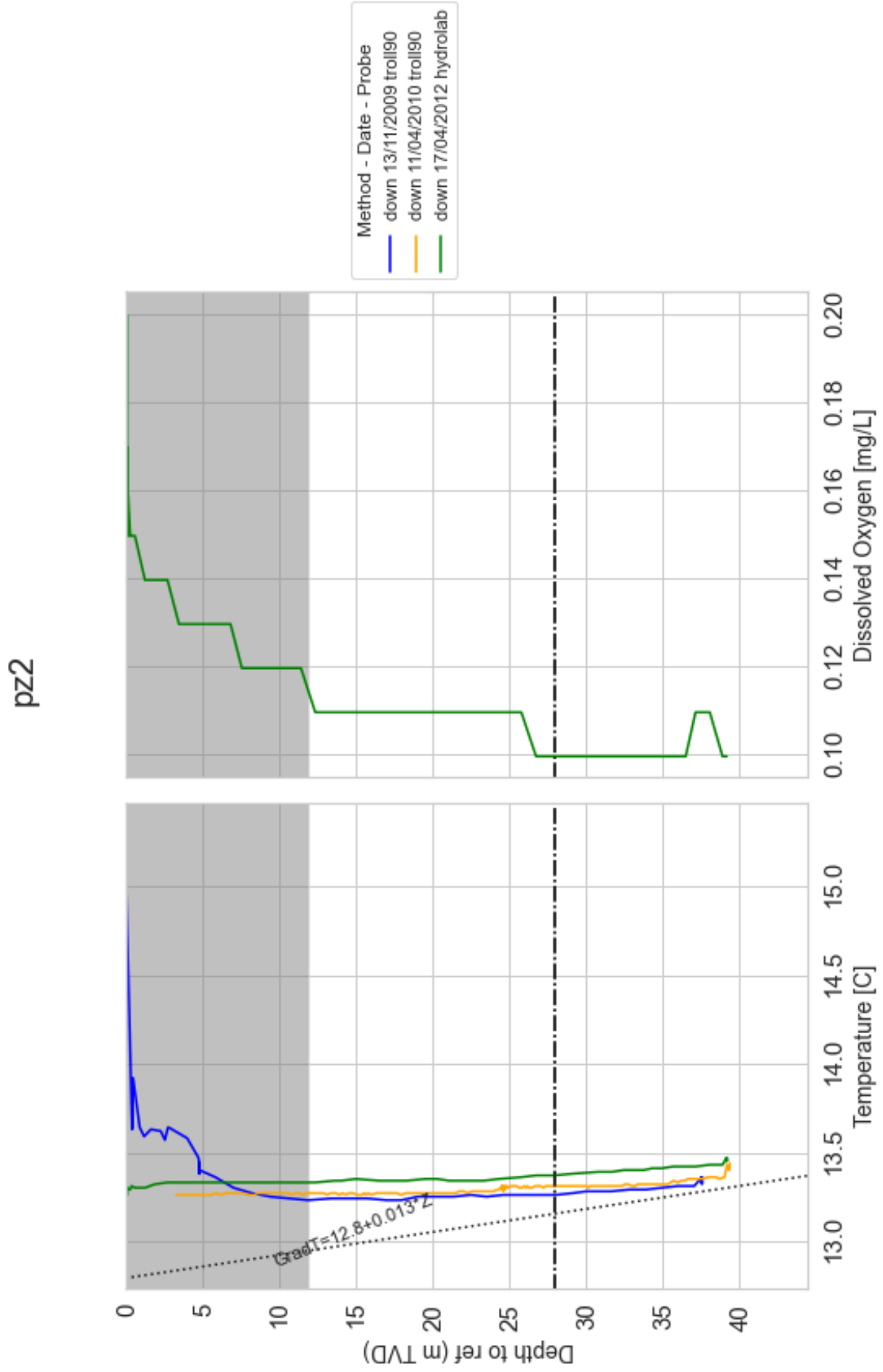


psr5

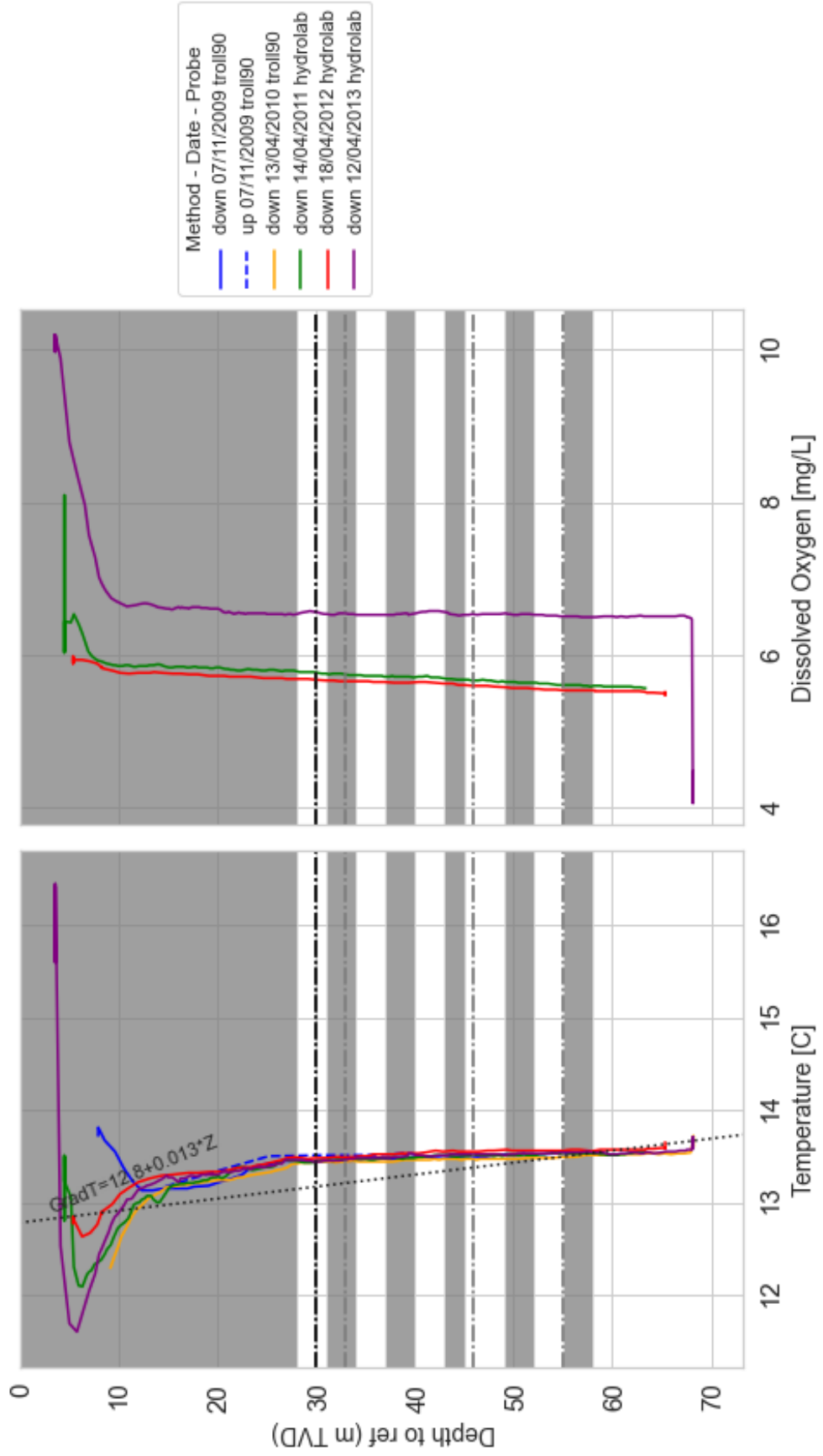


psr15

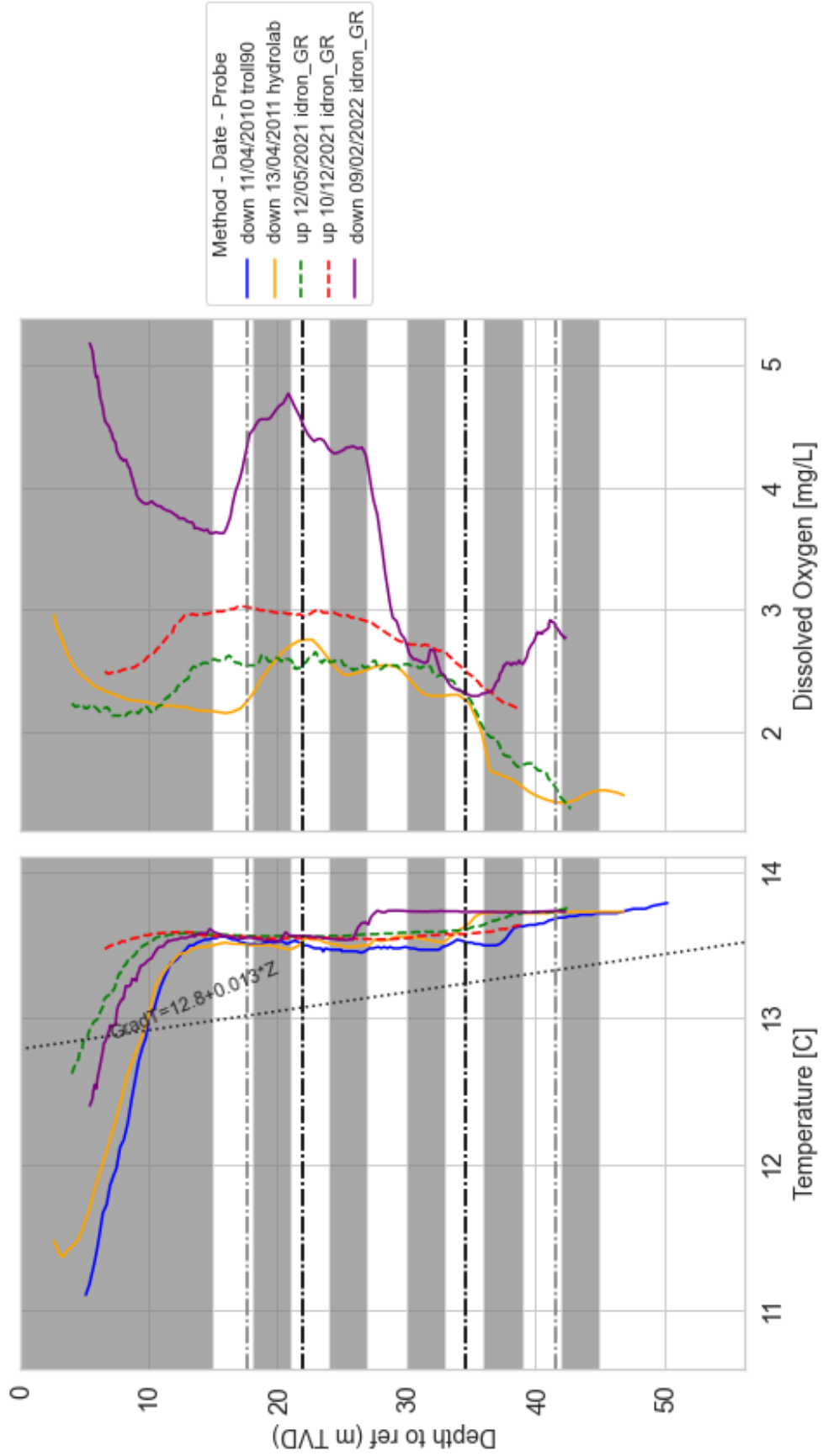


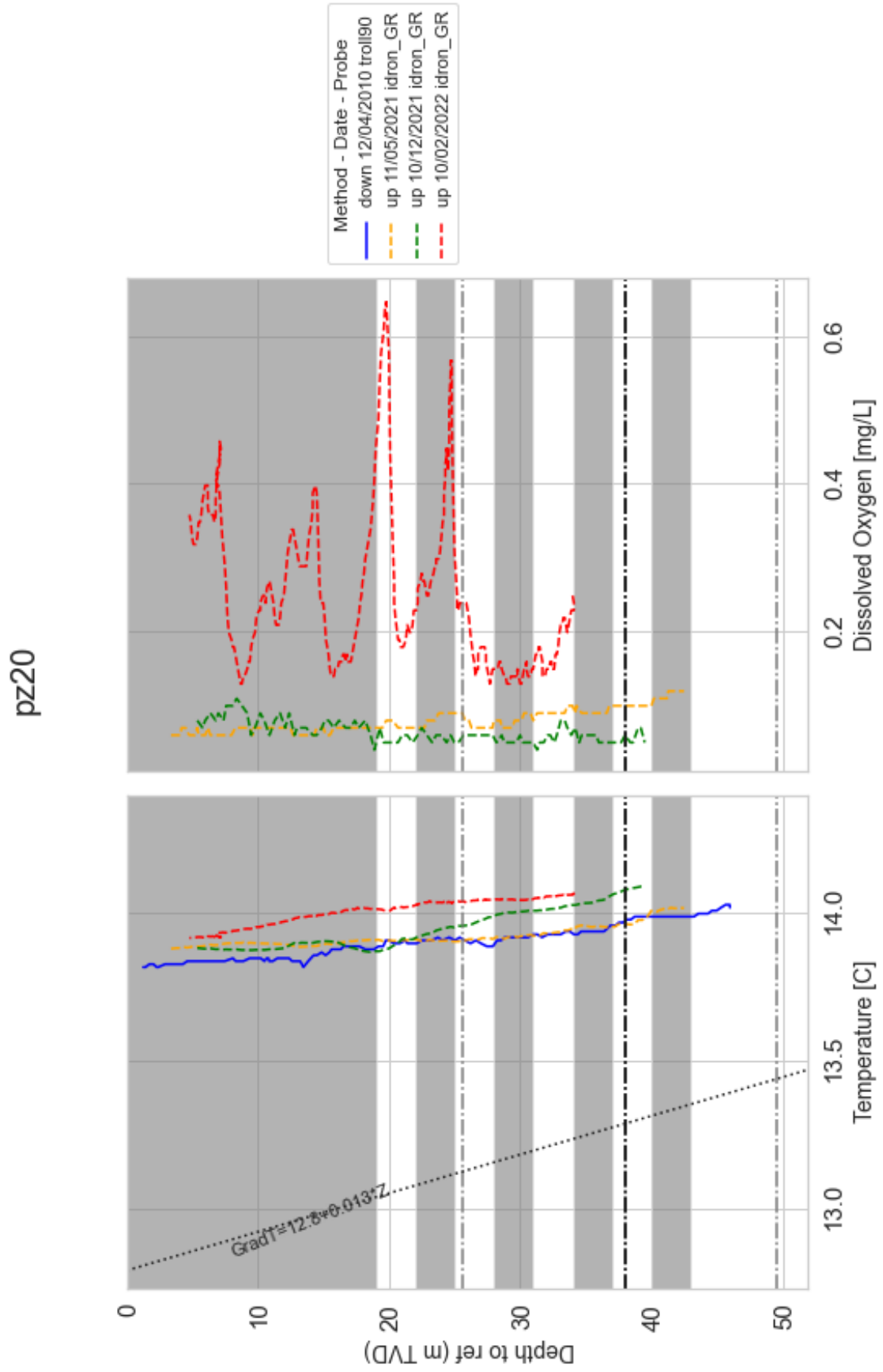


pz15

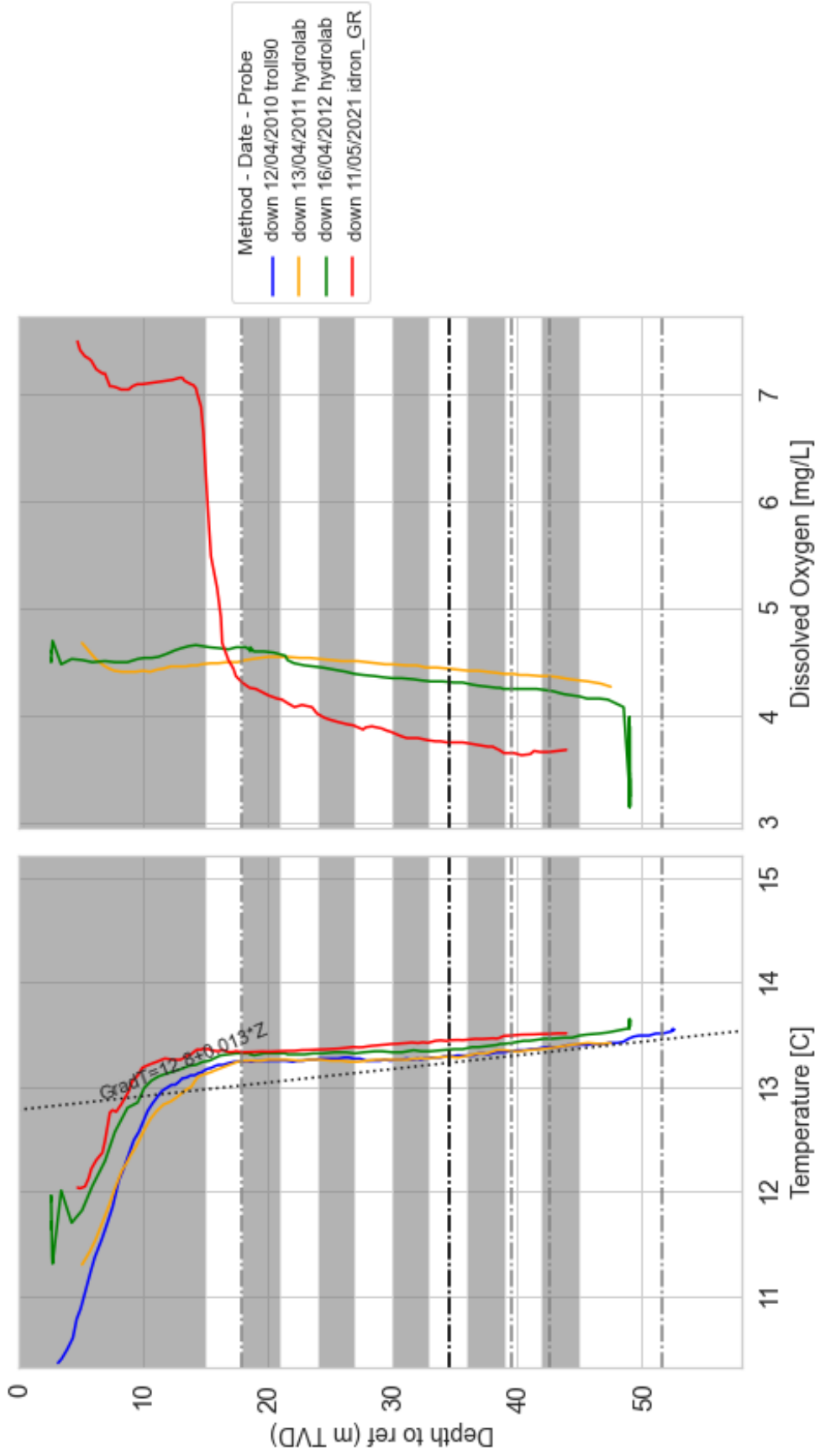


pz18

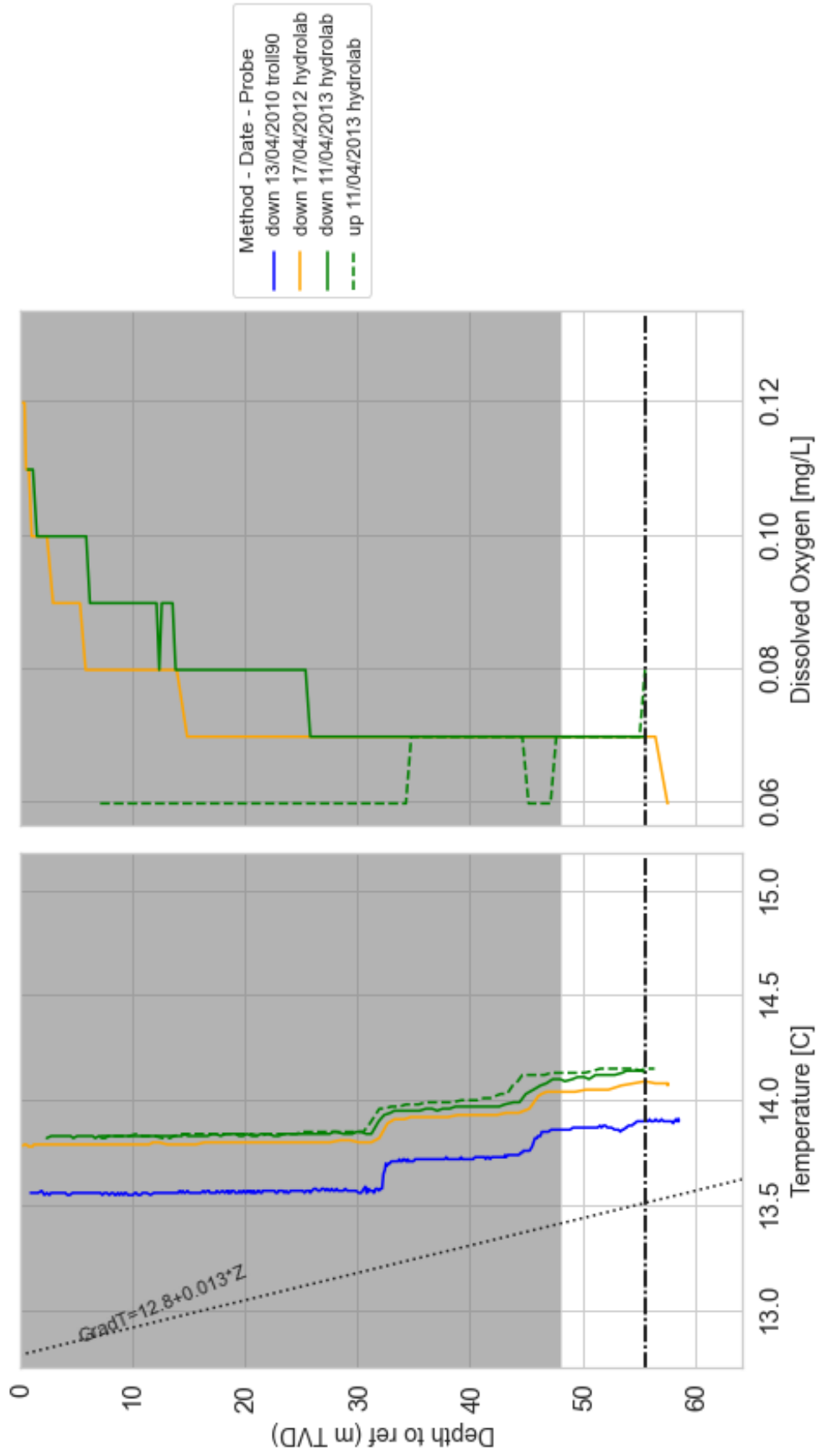




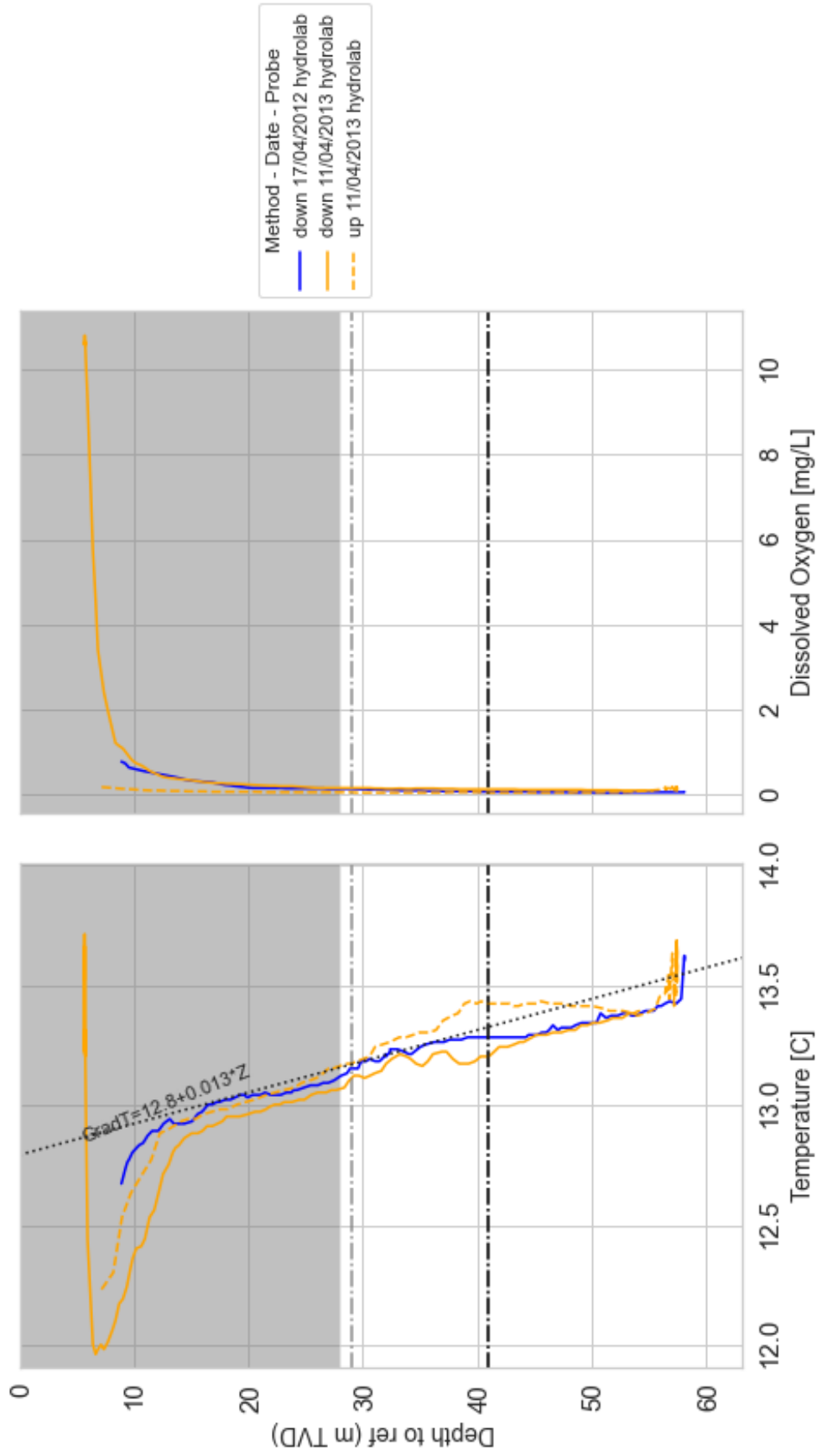
pz21



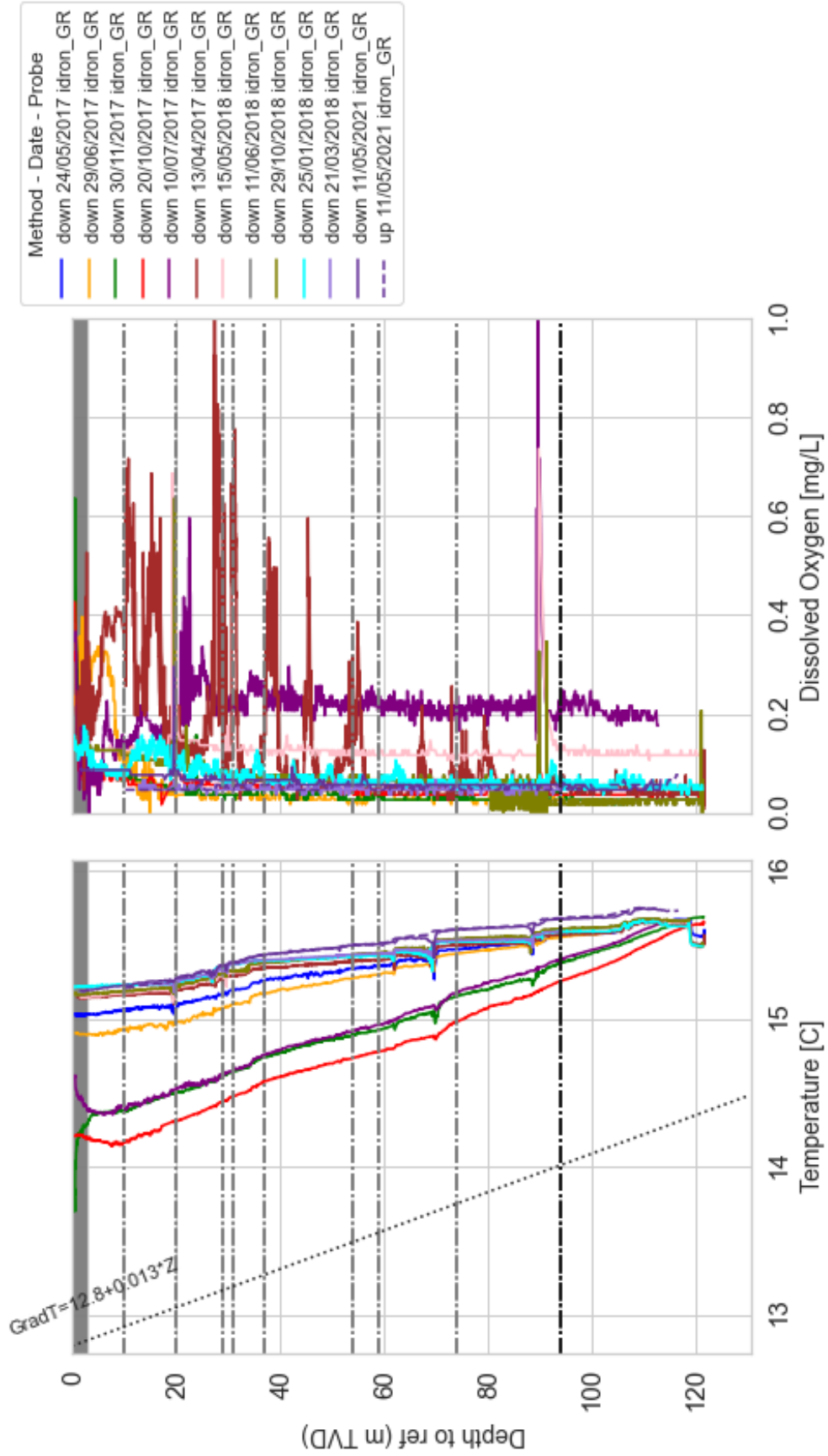
pz22



pz23



pz26



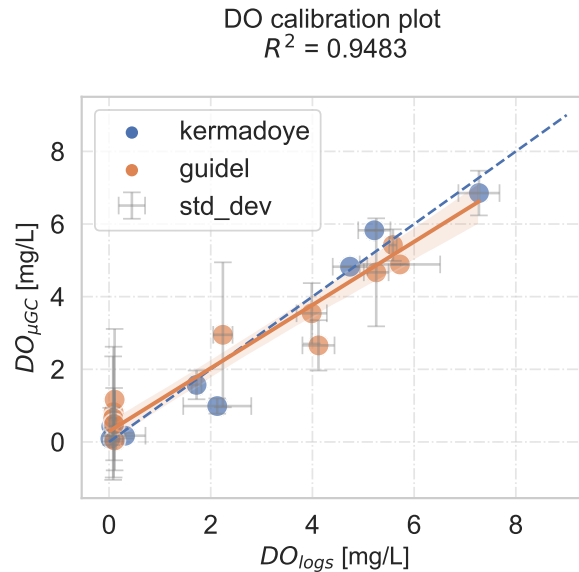


Figure 3. Calibration plot for DO measurements with the multiparameter probe (logs) vs gas chromatography (μGC) analysis made on the same samples.

References

84

- 85 Blanc, P., Lassin, A., Piantone, P., Azaroual, M., Jacquemet, N., Fabbri, A., &
86 Gaucher, E. C. (2012). Thermoddem: A geochemical database focused on
87 low temperature water/rock interactions and waste materials. *Applied Geo-*
88 *chemistry*, 27(10), 2107–2116. Retrieved from [http://dx.doi.org/10.1016/](http://dx.doi.org/10.1016/j.apgeochem.2012.06.002)
89 [j.apgeochem.2012.06.002](http://dx.doi.org/10.1016/j.apgeochem.2012.06.002) doi: 10.1016/j.apgeochem.2012.06.002
- 90 Bochet, O., Bethencourt, L., Dufresne, A., Farasin, J., Pédrot, M., Labasque, T.,
91 ... Le Borgne, T. (2020, feb). Iron-oxidizer hotspots formed by intermit-
92 tent oxic–anoxic fluid mixing in fractured rocks. *Nature Geoscience*, 13(2),
93 149–155. doi: 10.1038/s41561-019-0509-1
- 94 Klepikova, M. V., Le Borgne, T., Bour, O., & Davy, P. (2011). A methodology for
95 using borehole temperature–depth profiles under ambient, single and cross-
96 borehole pumping conditions to estimate fracture hydraulic properties. *Jour-*
97 *nal of Hydrology*, 407(1-4), 145–152. Retrieved from [http://dx.doi.org/](http://dx.doi.org/10.1016/j.jhydro.2011.07.018)
98 [10.1016/j.jhydro.2011.07.018](http://dx.doi.org/10.1016/j.jhydro.2011.07.018) doi: 10.1016/j.jhydro.2011.07.018
- 99 Le Borgne, T., Paillet, F., Bour, O., & Caudal, J. P. (2006). Cross-borehole flowme-
100 ter tests for transient heads in heterogeneous aquifers. *Ground Water*, 44(3),
101 444–452. doi: 10.1111/j.1745-6584.2005.00150.x
- 102 Palandri, J., & Kharaka, Y. (2004). *A Compilation of Rate Parameters of Water-*
103 *Mineral Interaction Kinetics* (Vol. REPORT 200; Tech. Rep.).
- 104 Pouladi, B., Bour, O., Longuevergne, L., de La Bernardie, J., & Simon, N. (2021).
105 Modelling borehole flows from Distributed Temperature Sensing data to
106 monitor groundwater dynamics in fractured media. *Journal of Hydrology*,
107 598(November 2020). doi: 10.1016/j.jhydro.2021.126450
- 108 Ruelleu, S., Moreau, F., Bour, O., Gapais, D., & Martelet, G. (2010). Impact of
109 gently dipping discontinuities on basement aquifer recharge: An example from
110 Ploemeur (Brittany, France). *Journal of Applied Geophysics*, 70(2), 161–168.
111 Retrieved from <http://dx.doi.org/10.1016/j.jappgeo.2009.12.007> doi:

